Supplementary Information for
Freeform Spectrally Stable Topological Photonic Vortex Resonators

Yuma Kawaguchi[1]*, Daria Smirnova[2]*, Filipp Komissarenko[1,3], Daria Kafeeva[1], Svetlana Kiriushechkina[1], Andrea Alu[5], Jeffery Allen[4], Monica Allen[4], and Alexander Khanikaev[3]

[1]Department of Electrical Engineering, The City College of New York, New York, NY 10031, USA
[2]Research School of Physics, The Australian National University, Canberra, ACT 2601, Australia
[3]College of Optics and Photonics – CREOL, University of Central Florida, Orlando, FL 32816, USA
[4]Air Force Research Laboratory, Munitions Directorate, Eglin AFB, Eglin, FL 32542, USA
[5]Advanced Science Research Center, City University of New York, New York, NY 10031, USA
*These authors contributed equally to the present manuscript

Table of Contents

Section A. Effective Dirac model

We follow the lines of derivation as presented in our work [1] to obtain the effective Hamiltonian for the dielectric slab metasurface patterned into holes with two types of geometric perturbation: staggering the sizes of the holes and hexameric clustering within a unit cell.

We consider a two-dimensional (2D) distorted honeycomb lattice constituting a triangular lattice of hexagons, see Fig. S1. The lattice vectors of the triangular lattice are chosen $\boldsymbol{a}_1 = a\,(0,1)$ and $\boldsymbol{a}_2 = a\left(\sqrt{3}/2, -1/2\right)$. In the sublattice (real-space) basis, six sites make up the unit cell (numbering is clockwise), and the six-component wavefunction is

$$\boldsymbol{\alpha} = (\alpha_1, \alpha_2, \alpha_3, \alpha_4, \alpha_5, \alpha_6)^T . \tag{S1}$$

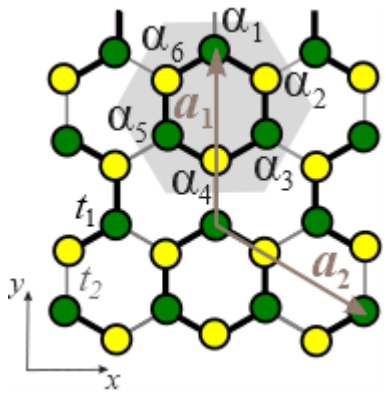

Fig. S1. Lattice schematic. Schematic representation of the tight-binding model (TBM) on a 2D triangular lattice formed by hexamer clusters. Black and grey lines depict intracell t_1 and intercell t_2 hoppings between the sites. The sites of two sublattices are painted by green and yellow circles. Shaded is one hexagonal unit cell.

The momentum space Hamiltonian $\widehat{H}(\boldsymbol{k})$ for this lattice reads

$$\widehat{H}(\boldsymbol{k}) = \begin{pmatrix} m_{VH} & -t_1 & 0 & -t_2\, e^{i\boldsymbol{k}\boldsymbol{a}_1} & 0 & -t_1 \\ -t_1 & -m_{VH} & -t_1 & 0 & -t_2\, e^{i\boldsymbol{k}(\boldsymbol{a}_1+\boldsymbol{a}_2)} & 0 \\ 0 & -t_1 & m_{VH} & -t_1 & 0 & -t_2\, e^{i\boldsymbol{k}\boldsymbol{a}_2} \\ -t_2\, e^{-i\boldsymbol{k}\boldsymbol{a}_1} & 0 & -t_1 & -m_{VH} & -t_1 & 0 \\ 0 & -t_2\, e^{-i\boldsymbol{k}(\boldsymbol{a}_1+\boldsymbol{a}_2)} & 0 & -t_1 & m_{VH} & -t_1 \\ -t_1 & 0 & -t_2 e^{-i\boldsymbol{k}\boldsymbol{a}_2} & 0 & -t_1 & -m_{VH} \end{pmatrix}, \tag{S2}$$

where m_{VH} quantifies a detuning between two sublattices, $t_{1,2}$ describe intra/intercell coupling. Around the Brillouin zone center at Γ point, $\boldsymbol{k} = 0$, Eq. (S2) reduces to

$$\widehat{H}(\boldsymbol{k}) \approx -\begin{pmatrix} -m_{VH} & t_1 & 0 & t_2\,(1 + i\,\boldsymbol{k}\boldsymbol{a}_1) & 0 & t_1 \\ t_1 & m_{VH} & t_1 & 0 & t_2\,(1 + i\boldsymbol{k}(\boldsymbol{a}_1 + \boldsymbol{a}_2)) & 0 \\ 0 & t_1 & -m_{VH} & t_1 & 0 & t_2\,(1 + i\boldsymbol{k}\boldsymbol{a}_2) \\ t_2\,(1 - i\,\boldsymbol{k}\boldsymbol{a}_1) & 0 & t_1 & m_{VH} & t_1 & 0 \\ 0 & t_2\,(1 - i\boldsymbol{k}(\boldsymbol{a}_1 + \boldsymbol{a}_2)) & 0 & t_1 & -m_{VH} & t_1 \\ t_1 & 0 & t_2(1 - i\boldsymbol{k}\boldsymbol{a}_2) & 0 & t_1 & m_{VH} \end{pmatrix}. \tag{S3}$$

Considering the condition that both t_1, t_2 weakly deviate from the coupling strength t in the unperturbed (graphene-like) lattice, $|t_1 - t_2| \ll |t|$ and $|m_{VH}| \ll t$, we perform a unitary transformation,

$$\hat{U} = \frac{1}{\sqrt{6}} \begin{pmatrix} i & -1 & -i & -1 & 1 & 1 \\ ie^{2i\pi/3} & -e^{i\pi/3} & -ie^{-2i\pi/3} & -e^{-i\pi/3} & -1 & 1 \\ ie^{-2i\pi/3} & -e^{2i\pi/3} & -ie^{2i\pi/3} & -e^{-2i\pi/3} & 1 & 1 \\ i & 1 & -i & 1 & -1 & 1 \\ ie^{2i\pi/3} & e^{i\pi/3} & -ie^{-2i\pi/3} & e^{-i\pi/3} & 1 & 1 \\ ie^{-2i\pi/3} & e^{2i\pi/3} & -ie^{2i\pi/3} & e^{-2i\pi/3} & -1 & 1 \end{pmatrix}, \tag{S4}$$

and obtain the Hamiltonian $\widehat{\mathcal{H}} = \hat{U}^{-1}\widehat{H}\hat{U}$ in a new basis $\mathbf{u} = \hat{U}^{-1}\boldsymbol{\alpha}$ as

$$\widehat{\mathcal{H}}(\boldsymbol{k}) = \begin{pmatrix} m_{SH} & v_D(-k_y + ik_x) & 0 & im_{VH} & v_D(k_y + ik_x) & 0 \\ v_D(-k_y - ik_x) & -m_{SH} & im_{VH} & 0 & 0 & v_D(k_x + ik_y) \\ 0 & -im_{VH} & m_{SH} & v_D(k_y + ik_x) & -v_D(k_y - ik_x) & 0 \\ -im_{VH} & 0 & v_D(k_y - ik_x) & -m_{SH} & 0 & -v_D(k_x - ik_y) \\ v_D(k_y - ik_x) & 0 & -v_D(k_y + ik_x) & 0 & 2t_1 + t_2 & m_{VH} \\ 0 & v_D(k_x - ik_y) & 0 & -v_D(k_x + ik_y) & m_{VH} & -2t_1 - t_2 \end{pmatrix}, \tag{S5}$$

where we denote the Dirac velocity $v_D = t_2 a/2$, and the mass term $m_{SH} = t_1 - t_2$. Because $|m_{VH}|$ and $|m_{SH}|$ are much smaller than $|2t_1 + t_2|$, we neglect the high-energy part of $\widehat{\mathcal{H}}$ and exclude the fifth and the sixth columns and rows describing singlet states. Thus, we obtain the effective Hamiltonian $\widehat{\mathcal{H}}_{\text{eff}}$ in the subspace of the circularly-polarized states $\mathbf{u} = (u_1, u_2, u_3, u_4)^T$ to the first order of k,

$$\widehat{\mathcal{H}}_{\text{eff}}(\boldsymbol{k}) = \begin{pmatrix} m_{SH} & v_D(-k_y + ik_x) & 0 & im_{VH} \\ v_D(-k_y - ik_x) & -m_{SH} & im_{VH} & 0 \\ 0 & -im_{VH} & m_{SH} & v_D(k_y + ik_x) \\ -im_{VH} & 0 & v_D(k_y - ik_x) & -m_{SH} \end{pmatrix} \tag{S6}$$

$$= m_{SH}\,\hat{\sigma}_z\,\hat{s}_0 - v_D\,k_y\,\hat{\sigma}_x\,\hat{s}_z - v_D\,k_x\,\hat{\sigma}_y\,\hat{s}_0 - m_{VH}\,\hat{\sigma}_x\,\hat{s}_y\,.$$

Its bulk spectrum $\omega_{\pm}(\boldsymbol{k})$ is gapped and consists of two doubly-degenerate bands,

$$\omega_{\pm}(\boldsymbol{k}) = \pm\sqrt{m_{SH}^2 + m_{VH}^2 + v_D^2(k_x^2 + k_y^2)}. \tag{S7}$$

In the $\mathbf{u}$ basis, $u_{2,4}/u_{1,3}$ represent to the dipolar and quadrupolar components, respectively.

With the transformation

$$\hat{U}_{\text{ab}} = \frac{1}{\sqrt{2}} \begin{pmatrix} 0 & i & -i & 0 \\ 1 & 0 & 0 & 1 \\ 0 & i & i & 0 \\ -1 & 0 & 0 & 1 \end{pmatrix} \tag{S8}$$

to the basis $\mathbf{u}_{ab} = (u_b, u_a, v_a, v_b)^T = \hat{U}_{\text{ab}}(u_1, u_2, u_3, u_4)^T$, $\widehat{\mathcal{H}}_{\text{eff}}$ can also be rewritten in the form

$$\widehat{\mathcal{H}}_{ab}(\boldsymbol{k}) = \begin{pmatrix} 0 & v_D(k_x - ik_y) & -(m_{SH} - im_{VH}) & 0 \\ v_D(k_x + ik_y) & 0 & 0 & -(m_{SH} - im_{VH}) \\ -(m_{SH} + im_{VH}) & 0 & 0 & v_D(-k_x + ik_y) \\ 0 & -(m_{SH} + im_{VH}) & v_D(-k_x - ik_y) & 0 \end{pmatrix} \tag{S9}$$

$$= v_D(\hat{\sigma}_x k_x + \hat{\sigma}_y k_y)\hat{\tau}_z - \hat{\sigma}_0(m_{SH}\hat{\tau}_x + m_{VH}\hat{\tau}_y).$$

If the two effective masses (spin-Hall m_{SH} and valley-Hall m_{VH}) are parametrised by the same real-valued phase, such as $m_{SH} = m_0 \cos\varphi$, $m_{VH} = m_0 \sin\varphi$, they can be combined into a single complex-valued quantity in the complex plane $m(\rho, \varphi) = m_0 e^{-i\varphi}$, similar to the momentum in the polar coordinate system $k_x \mp ik_y = ke^{\mp i\varphi}$:

$$\widehat{\mathcal{H}}_{ab}(\boldsymbol{k}) = \begin{pmatrix} 0 & v_D k e^{-i\varphi} & -m_0 e^{-i\varphi} & 0 \\ v_D k e^{i\varphi} & 0 & 0 & -M_0 e^{-i\varphi} \\ -m_0 e^{i\varphi} & 0 & 0 & -v_D k e^{-i\varphi} \\ 0 & -m_0 e^{i\varphi} & -v_D k e^{i\varphi} & 0 \end{pmatrix} \tag{S10}$$
$$= v_D\big(\hat{\sigma}_x k_x + \hat{\sigma}_y k_y\big)\hat{\tau}_z - m_0\hat{\sigma}_0\big(\cos\varphi\,\hat{\tau}_x + \sin\varphi\,\hat{\tau}_y\big).$$

Extended 3D parameter space spanned by three masses

If, additionally, the intracell coupling dimerization $t_1 \neq t_3$ is present in the lattice Fig. S1, the full lattice Hamiltonian Eq. (S2) is modified to

$$\widehat{H}(\boldsymbol{k}) = \begin{pmatrix} m_{VH} & -t_1 & 0 & -t_2 e^{i\boldsymbol{k}\boldsymbol{a}_1} & 0 & -t_3 \\ -t_1 & -m_{VH} & -t_3 & 0 & -t_2 e^{i\boldsymbol{k}(\boldsymbol{a}_1+\boldsymbol{a}_2)} & 0 \\ 0 & -t_3 & m_{VH} & -t_1 & 0 & -t_2 e^{i\boldsymbol{k}\boldsymbol{a}_2} \\ -t_2\, e^{-i\boldsymbol{k}\boldsymbol{a}_1} & 0 & -t_1 & -m_{VH} & -t_3 & 0 \\ 0 & -t_2 e^{-i\boldsymbol{k}(\boldsymbol{a}_1+\boldsymbol{a}_2)} & 0 & -t_3 & m_{VH} & -t_1 \\ -t_3 & 0 & -t_2 e^{-i\boldsymbol{k}\boldsymbol{a}_2} & 0 & -t_1 & -m_{VH} \end{pmatrix}, \tag{S11}$$

and the effective Hamiltonian at small $\boldsymbol{k}$, which is a generalized version of Eq. (S6), reduces to

$$\widehat{\mathcal{H}}_{\text{eff}}(\boldsymbol{k}) = \begin{pmatrix} m_{SH} & v_D(-k_y + ik_x) & 0 & im_{VH} + m_{KK} \\ v_D(-k_y - ik_x) & -m_{SH} & im_{VH} + m_{KK} & 0 \\ 0 & -im_{VH} + m_{KK} & m_{SH} & v_D(k_y + ik_x) \\ -im_{VH} + m_{KK} & 0 & v_D(k_y - ik_x) & -m_{SH} \end{pmatrix}, \tag{S12}$$

where we denote $m_{KK} = \sqrt{3}(t_3 - t_1)/2$ proportional to the coupling difference $(t_3 - t_1)$. The bulk spectrum of (S9) is then

$$\omega_{\pm}(\boldsymbol{k}) = \pm\sqrt{m_{SH}^2 + m_{VH}^2 + m_{KK}^2 + v_D^2\big(k_x^2 + k_y^2\big)}. \tag{S13}$$

All together, three masses span a 3D parameter space $(m_{SH}, m_{VH}, m_{KK}) = m_0(\cos\Theta, \sin\Theta\cos\Phi, \sin\Theta\sin\Phi)$. In Ref. [1], we operated in the 2D parameter subspace spanned by valley-Hall and spin-Hall masses that form a circle on the Poincare sphere. In our notations for edge state transformations, Θ varied along the interface and $\Phi = 0$ was fixed, and we described how the polarisation (pseudo-spin) of bulk and edge modes evolves adiabatically, giving rise to a geometric phase.

Here, we generalize our approach to cover all possible polarization states on the Poincaré sphere. For this purpose, we change the basis s $\boldsymbol{\psi} = \hat{U}_3\boldsymbol{u}$, using the transformation $\hat{U}_3$ that diagonalizes the mass matrix. For instance, a useful form for obtaining the defect state bound to the mass vortex in the sublattice basis is given by (obtained with $\widehat{U}_{\text{ab}}$ (S8), where the last row is multiplied by (-1)):

$$\begin{aligned}\widehat{\mathcal{H}}_{\mathrm{eff}\,2} &= v_D\left(\hat{\sigma}_x k_x + \hat{\sigma}_y k_y\right)\hat{\tau}_0 - \hat{\sigma}_z\left(m_{SH}\hat{\tau}_x + m_{VH}\hat{\tau}_y\right) - \hat{\sigma}_z\hat{\tau}_z m_{KK} \\ &= v_D k_x\hat{\Gamma}_1 + v_D k_y\hat{\Gamma}_2 - m_{SH}\hat{\Gamma}_3 - m_{VH}\hat{\Gamma}_4 - m_{KK}\hat{\Gamma}_5,\end{aligned} \tag{S14}$$

where we introduced 4×4 matrices $\hat{\Gamma}_i, i = 1, \ldots, 5$ satisfying the anticommutation relation $\hat{\Gamma}_i\hat{\Gamma}_j = 2\delta_{ij}I_{4\times4}$ similar to 2×2 Pauli matrices in the two-band Dirac Hamiltonian, $\left(\hat{\Gamma}_1, \hat{\Gamma}_2, \hat{\Gamma}_3, \hat{\Gamma}_4, \hat{\Gamma}_5\right) = \left(\hat{\sigma}_x\hat{\tau}_0, \hat{\sigma}_y\hat{\tau}_0, \hat{\sigma}_z\hat{\tau}_x, \hat{\sigma}_z\hat{\tau}_y, \hat{\sigma}_z\hat{\tau}_z\right)$. We directly take (S12) with the mass matrix derived above from TBM to obtain the Hamiltonian $\widehat{\mathcal{H}}_{\mathrm{eff}\,3} = \hat{U}\widehat{\mathcal{H}}_{\mathrm{eff}}\hat{U}^{-1}$ for $\boldsymbol{\psi}$ in the form

$$\widehat{\mathcal{H}}_{\mathrm{eff}\,3}(\boldsymbol{k}) = \begin{pmatrix} m_0 & 0 & 0 & v_D\left(k_y + ik_x\right) \\ 0 & m_0 & v_D\left(k_y - ik_x\right) & 0 \\ 0 & v_D\left(k_y + ik_x\right) & -m_0 & 0 \\ v_D\left(k_y - ik_x\right) & 0 & 0 & -m_0 \end{pmatrix} \tag{S15}$$

that consists of two decoupled blocks for $(\psi_1, \psi_4)^T$ and $(\psi_2, \psi_3)^T$. The generalised transformation matrix $\hat{U}_3(\Theta, \Phi)$ reads

$$\hat{U}_3 = \begin{pmatrix} 0 & -ie^{i\Phi}\sin\frac{\Theta}{2} & \cos\frac{\Theta}{2} & 0 \\ -ie^{i\Phi}\cos\frac{\Theta}{2} & 0 & 0 & \sin\frac{\Theta}{2} \\ 0 & ie^{i\Phi}\cos\frac{\Theta}{2} & \sin\frac{\Theta}{2} & 0 \\ ie^{i\Phi}\sin\frac{\Theta}{2} & 0 & 0 & \cos\frac{\Theta}{2} \end{pmatrix}. \tag{S16}$$

The bulk modes of the Hamiltonian $\widehat{\mathcal{H}}_{\mathrm{eff}\,3}$ are doubly degenerate, with eigenfrequencies $\omega_\pm = \pm\sqrt{m_0^2 + k_x^2 + k_y^2}$, rewritten from (S13). For edge states at the mass-inverted interface ($m_0(y > 0) = m_c > 0$ and $m_0(y < 0) = -m_c < 0$, where $m_c = \mathrm{const}$), with the ansatz $\propto \exp\left(ik_x x - \kappa|y|\right), k_y = i\varkappa$ at $y > 0$, and $k_y = -i\varkappa$ at $y < 0$, where $\varkappa > 0$ is the decay rate, we find the localization rate $\varkappa^2 = m_c^2$. They are spin-momentum-locked: left-propagating wave $k_x = -\omega$ of polarization $(\psi_1, 0, 0, \psi_4)^T = 1/\sqrt{2}(1,0,0,i)^T$, and right-propagating wave $k_x = \omega$ of polarization $(0, \psi_2, \psi_3, 0)^T = 1/\sqrt{2}(0,1,i,0)^T$. The $\boldsymbol{\psi}$ and $\boldsymbol{u}$ vectors are related via the transformation $\boldsymbol{u} = {\hat{U}_3}^{-1}\boldsymbol{\psi}$:

$${\hat{U}_3}^{-1} = \begin{pmatrix} 0 & ie^{-i\Phi}\cos\frac{\Theta}{2} & 0 & -ie^{-i\Phi}\sin\frac{\Theta}{2} \\ ie^{-i\Phi}\sin\frac{\Theta}{2} & 0 & -ie^{-i\Phi}\cos\frac{\Theta}{2} & 0 \\ \cos\frac{\Theta}{2} & 0 & \sin\frac{\Theta}{2} & 0 \\ 0 & \sin\frac{\Theta}{2} & 0 & \cos\frac{\Theta}{2} \end{pmatrix}, \tag{S17}$$

$$\boldsymbol{u} = \begin{pmatrix} ie^{-i\Phi}\left(\psi_2 \cos\frac{\Theta}{2} - \psi_4 \sin\frac{\Theta}{2}\right) \\ ie^{-i\Phi}\left(\psi_1 \sin\frac{\Theta}{2} - \psi_3 \cos\frac{\Theta}{2}\right) \\ \psi_1 \cos\frac{\Theta}{2} + \psi_3 \sin\frac{\Theta}{2} \\ \psi_2 \sin\frac{\Theta}{2} + \psi_4 \cos\frac{\Theta}{2} \end{pmatrix}. \tag{S18}$$

The polarization vectors for the right- (I) and left- (II) propagating edge states, which can be launched at $\Theta = 0, \Phi = 0$ at the input and evolve adiabatically, are as follows

$$\boldsymbol{u}_{\text{e.s. I}} = \frac{1}{\sqrt{2}} \begin{pmatrix} ie^{-i\Phi}\cos(\Theta/2) \\ e^{-i\Phi}\cos(\Theta/2) \\ i\sin(\Theta/2) \\ \sin(\Theta/2) \end{pmatrix}, \tag{S19}$$

$$\boldsymbol{u}_{\text{e.s. II}} = \frac{1}{\sqrt{2}} \begin{pmatrix} e^{-i\Phi}\cos(\Theta/2) \\ ie^{-i\Phi}\sin(\Theta/2) \\ \cos(\Theta/2) \\ i\cos(\Theta/2) \end{pmatrix}. \tag{S20}$$

Section B. Vortex-mass Jackiw-Rebbi bound state

The eigenvalue problem with the Hamiltonian (S6) (setting $m_{KK} = 0$), $\widehat{\mathcal{H}}_{\text{eff}}(\boldsymbol{k})\mathbf{u} = \omega\mathbf{u}$, on substitution of spatial operators $\boldsymbol{k} = (k_x, k_y) = -i(\partial_x, \partial_y)$, represents a system of partial differential equations (PDEs) for $\mathbf{u}$

$$\begin{pmatrix} m_{SH} & v_D(i\partial_y + \partial_x) & 0 & im_{VH} \\ v_D(i\partial_y - \partial_x) & -m_{SH} & im_{VH} & 0 \\ 0 & -im_{VH} & m_{SH} & v_D(-i\partial_y + \partial_x) \\ -im_{VH} & 0 & v_D(-i\partial_y - \partial_x) & -m_{SH} \end{pmatrix} \mathbf{u} = \omega\mathbf{u}, \tag{S21}$$

that can be solved numerically in the xy plane. Specifically, for a single-vortex cavity problem with continuous [2] or discrete [3] phase modulation implementing the mass winding, the mass profile profile $m_0(\rho)$ in (S11) is a radial function in the polar coordinate system (ρ, φ), or a constant. In this Section, we provide the solution for the particular case of a vortex-like mass distribution of the form $m(\rho, \varphi) = m_0 e^{iQ\varphi}$, with the negative unity charge $Q = -1$, as in (S10), and $m_0 = m_{\text{c}} = \text{const}$.

In the sublattice basis $\mathbf{u}_{ab}$, adopting the spatial-derivative operator in the polar coordinates in Eqs. (S10),

$$ke^{\mp i\varphi} = -ie^{\mp i\varphi}\left(\frac{\partial}{\partial\rho} \mp \frac{i}{\rho}\frac{\partial}{\partial\varphi}\right), \tag{S22}$$

the eigenvalue problem for the four-component vector $\mathbf{u}_{ab} = (u_b, u_a, v_a, v_b)^T$ reads

$$\begin{pmatrix} -\omega & -iv_D e^{-i\varphi}\left(\frac{\partial}{\partial\rho}-\frac{i}{\rho}\frac{\partial}{\partial\varphi}\right) & -m_c e^{-i\varphi} & 0 \\ -ie^{i\varphi}\left(\frac{\partial}{\partial\rho}+\frac{i}{\rho}\frac{\partial}{\partial\varphi}\right) & -\omega & 0 & -m_c e^{-i\varphi} \\ -m_c e^{i\varphi} & 0 & -\omega & iv_D e^{-i\varphi}\left(\frac{\partial}{\partial\rho}-\frac{i}{\rho}\frac{\partial}{\partial\varphi}\right) \\ 0 & -m_c e^{i\varphi} & ie^{i\varphi}\left(\frac{\partial}{\partial\rho}+\frac{i}{\rho}\frac{\partial}{\partial\varphi}\right) & -\omega \end{pmatrix}\begin{pmatrix} u_b \\ u_a \\ v_a \\ v_b \end{pmatrix} = 0. \tag{S23}$$

In the following we set the velocity parameter $v_D = 1$. The system (S23) represents an eigenvalue problem for the modes of the cavity created by the inhomogeneous distribution of the off-diagonal mass terms $m(\rho,\varphi)$ and $m^*(\rho,\varphi)$. The eigenfunctions $[u_b, u_a, v_a, v_b]$ should be finite at $\rho = 0$ and decay at infinity $\rho \to \infty$.

Rearranging (S23) leads to

$$\begin{aligned} \left(\frac{\partial}{\partial\rho}-\frac{i}{\rho}\frac{\partial}{\partial\varphi}\right)u_a - im_c v_a &= i\omega u_b e^{i\varphi}, \\ -im_c u_a - \left(\frac{\partial}{\partial\rho}+\frac{i}{\rho}\frac{\partial}{\partial\varphi}\right)v_a &= i\omega v_b e^{-i\varphi}, \\ \left(\frac{\partial}{\partial\rho}+\frac{i}{\rho}\frac{\partial}{\partial\varphi}\right)u_b - im_c e^{-2i\varphi}v_b &= i\omega u_a e^{-i\varphi}, \\ -im_c e^{2i\varphi}u_b - \left(\frac{\partial}{\partial\rho}-\frac{i}{\rho}\frac{\partial}{\partial\varphi}\right)v_b &= i\omega v_a e^{i\varphi}. \end{aligned} \tag{S24}$$

The immediate analytical solution of Eqs. (S24) is pinned to the zero frequency $\omega = 0$. It is axially-symmetric, $\partial_\varphi = 0$, and resides at one a-sublattice (obtained by solving the first two equations of the system (S24)), with $v_b = u_b = 0$ and the decay scale $|m_c|^{-1}$ inversely proportional to the bandgap size in the bulk spectrum (S7):

$$\begin{pmatrix} u_b \\ u_a \\ v_a \\ v_b \end{pmatrix}(\rho,\varphi) \propto \frac{1}{\sqrt{2}}\begin{pmatrix} 0 \\ e^{-i\pi/4} \\ e^{i\pi/4} \\ 0 \end{pmatrix} e^{-|m_c|\rho}. \tag{S25}$$

Here, $u_a = v_a^*$. The host sublattice a/b depends on the rotation direction (chirality) in the mass vortex and corresponds to the negative or positive sign of the charge $Q = \mp 1$, respectively.

Transforming the eigenvector to the original basis of circularly-polarized states $\boldsymbol{u}(\omega = 0) = \widehat{U}_{\mathrm{ab}}^{-1}\boldsymbol{u}_{ab}(\omega = 0)$, we obtain all 4 nonzero components that describe the coupled spins:

$$\begin{pmatrix} u_1 \\ u_2 \\ u_3 \\ u_4 \end{pmatrix}(\rho,\varphi) \propto \frac{1}{2}\begin{pmatrix} 1 \\ 1 \\ 1 \\ 1 \end{pmatrix} f(\rho). \tag{S26}$$

Thus, it has a clear connection to the zero-energy edge states, – two spin-polarised edge states coexist at the same $\omega = 0$ at $k = 0$ and get coupled.

The solution (S25) is also consistent with definitions of the rotation operators for the Hamiltonian (S10). The rotation operator for one spin block in graphene (2×2 k-dependent Dirac block in (S10)), if rotated with respect to the axis directed out-of-plane by angle φ, is governed by $\hat{\sigma}$ matrices:

$$e^{-i(\varphi/2)\hat{\sigma}_z} = \cos(\varphi/2)\hat{\sigma}_0 - i\sin(\varphi/2)\hat{\sigma}_z = \begin{pmatrix} e^{-i\varphi/2} & 0 \\ 0 & e^{i\varphi/2} \end{pmatrix}. \quad \text{(S27)}$$

Under 2π rotation, the eigenstates acquire a π phase factor. Therefore, the eigenvectors need to be rotated twice to return in phase. Similarly, the rotation operators for Hamiltonian (S10) are given by matrix exponentials:

$$\hat{R}_M(\varphi) = e^{-i(\varphi/2)\hat{\tau}_z} = \cos\left(\frac{\varphi}{2}\right)\hat{\tau}_0 - i\sin\left(\frac{\varphi}{2}\right)\hat{\tau}_z = \begin{pmatrix} e^{-\frac{i\varphi}{2}} & 0 & 0 & 0 \\ 0 & e^{-\frac{i\varphi}{2}} & 0 & 0 \\ 0 & 0 & e^{\frac{i\varphi}{2}} & 0 \\ 0 & 0 & 0 & e^{\frac{i\varphi}{2}} \end{pmatrix}, \quad \text{(S28)}$$

$$\hat{R}_k(\varphi) = \begin{pmatrix} e^{-i\varphi/2} & 0 & 0 & 0 \\ 0 & e^{i\varphi/2} & 0 & 0 \\ 0 & 0 & e^{-i\varphi/2} & 0 \\ 0 & 0 & 0 & e^{i\varphi/2} \end{pmatrix}. \quad \text{(S29)}$$

The total rotation in an enclosed circular path is given by their multiplication

$$\hat{R}_k(\varphi)\hat{R}_M(\varphi) = \begin{pmatrix} e^{-i\varphi} & 0 & 0 & 0 \\ 0 & 1 & 0 & 0 \\ 0 & 0 & 1 & 0 \\ 0 & 0 & 0 & e^{i\varphi} \end{pmatrix}. \quad \text{(S30)}$$

Thus, the axially symmetric solution (S25) (its angular momentum is zero) has the first and last components equal to zero, $v_b = u_b = 0$, while u_a and v_a are angle-independent.

Section C. Line-defect cavity in the continuum Dirac description

Next, we consider a hybrid line defect, which consists of a line segment of the domain wall, with step-like mass change $m_{SH}(|x| < \rho_0, y > 0) = m_c$, $m_{SH}(|x| < \rho_0, y < 0) = -m_c$, $m_{VH}(|x| < \rho_0, y) = 0$ across the interface $y = 0$, and two side-attached mass semivortices $m(|x| > \rho_0) = m_c e^{i\left(\varphi - \frac{\pi}{2}\right)}$, whose centers are shifted to $(\pm\rho_0, 0)$ (see Fig. S2). In the middle region, within the straight-line interval $|x| < \rho_0$, the field in this cavity can be decomposed into contra-propagating spin-polarized edge waves confined to the horizontal spin-Hall domain wall. The polarization eigenvectors for spin-up and spin-down edge states are

$$(u_1, u_2, u_3, u_4)^T_{(+x)} = (1, -i, 0, 0)^T/\sqrt{2} \text{ for } k_x = \omega/v_D, \quad \text{(S31)}$$

$$(u_1, u_2, u_3, u_4)^T_{(-x)} = (0, 0, 1, i)^T/\sqrt{2} \text{ for } k_x = -\omega/v_D. \quad \text{(S32)}$$

The quantization of the wavenumber (and the corresponding eigenfrequencies of the cavity modes) follows from the boundary conditions, imposing the four-component wave function continuity at $x = \pm\rho_0$. The simplest solution at $\omega = 0$ is uniform along x, with $k_x = 0$, and exponentially localized in the y direction, $e^{-|m_c y|}$ for $|x| \le \rho_0$. It has two vanishing components $u_a = v_a = 0$, and matches the vortex-mass solution of the form $(u_b, u_a, v_a, v_b)^T(\rho) = e^{-|m_c|\rho}(1, 0, 0, -1)^T/\sqrt{2}$ with the solution center shifted to $(x, y) = (\pm\rho_0, 0)$. The corresponding polarization eigenvector is also consistent with representation of the reflection matrix in terms of the rotation matrices introduced above:

$$\hat{U}_{\mathrm{ab}}^{-1}\begin{pmatrix}u_b\\u_a\\v_a\\v_b\end{pmatrix}(\omega=0)=\frac{1}{\sqrt{2}}\hat{U}_{\mathrm{ab}}^{-1}\begin{pmatrix}1\\0\\0\\-1\end{pmatrix}=\frac{1}{2}\begin{pmatrix}1\\-i\\i\\-1\end{pmatrix}=\begin{pmatrix}u_1\\u_2\\u_3\\u_4\end{pmatrix}(\omega=0,|x|<\rho_0)\propto\frac{1}{\sqrt{2}}\begin{pmatrix}1\\-i\\0\\0\end{pmatrix}+\frac{i}{\sqrt{2}}\begin{pmatrix}0\\0\\1\\i\end{pmatrix} \quad \text{(S33)}$$

$$=\frac{1}{\sqrt{2}}\left(1+\hat{U}_{\mathrm{ab}}^{-1}\hat{R}_M(-\pi)\hat{R}_k(-\pi)\hat{U}_{\mathrm{ab}}\right)\begin{pmatrix}1\\-i\\0\\0\end{pmatrix}.$$

Reflection from the semivortex edge flips the spin, as required for the backward propagation, and introduces a phase shift of $\left(\pm\frac{\pi}{2}\right)$, being interpreted as rotation $\hat{R}_M(-\pi)\hat{R}_k(-\pi)$ over a semi-circle of infinitely small radius at the semivortex core. It implies mutual transformation of two spin-polarised edge waves upon reflections from the opposite vertical boundaries at $x=\pm\rho_0$.

The effective reflection matrices, related to the spinor boundary conditions at $x=\pm\rho_0$, can be used to approximate the bound-state quantisation for this line-defect cavity. This approximation adequately holds in the low-frequency regime, $\omega\approx 0$, and for high-frequency states, $\omega\to\pm m_{\mathrm{c}}$. By symmetry, the higher-order modes have pair-wise symmetric cos- or antisymmetric sin-like distributions of the components $v_b=-u_b$ and $u_a=v_a$, along the domain wall,

$$\begin{pmatrix}u_1\\u_2\\u_3\\u_4\end{pmatrix}\propto\frac{1}{\sqrt{2}}\begin{pmatrix}1\\-i\\0\\0\end{pmatrix}e^{ik_xx}\pm\frac{i}{\sqrt{2}}\begin{pmatrix}0\\0\\1\\i\end{pmatrix}e^{-ik_xx}, \quad \text{(S34)}$$

$$\begin{pmatrix}u_b\\u_a\\v_a\\v_b\end{pmatrix}\propto\frac{1}{\sqrt{2}}\begin{pmatrix}\cos k_xx\\i\sin k_xx\\i\sin k_xx\\-\cos k_xx\end{pmatrix}\text{ or }\begin{pmatrix}u_b\\u_a\\v_a\\v_b\end{pmatrix}\propto\frac{1}{\sqrt{2}}\begin{pmatrix}i\sin k_xx\\\cos k_xx\\\cos k_xx\\-i\sin k_xx\end{pmatrix}. \quad \text{(S35)}$$

Thus, in the limit of the long line, $\rho_0\gg(m_{\mathrm{c}}/v_D)$, the mode quantisation is approximated as $\omega(n)\approx v_Dk_x(n)\approx\frac{v_D}{\rho_0}\frac{\pi}{2}n$, with integer numbers $n=0,\pm1,\pm2$ ... The spectrum contains a robust zero-frequency mode, analogous to that in the free-form geometric-phase topological resonators [4].

Another representative line-defect configuration consists of a valley-Hall domain wall segment with the mass profile $m_{VH}(|x|<\rho_0,y>0)=-m_{\mathrm{c}}$, $m_{VH}(|x|<\rho_0,y<0)=m_{\mathrm{c}}$, $m_{SH}(|x|<\rho_0,y)=0$ and two side-attached semivortices $m(|x|>\rho_0)=m_{\mathrm{c}}e^{i\varphi}$. Two contra-propagating edge waves at the valley-Hall domain wall $|x|<\rho_0$ in the $\boldsymbol{u}$ basis are

$$(u_1,u_2,u_3,u_4)^T_{(+x)}=e^{-i\pi/4}(1,-i,-1,i)^T/2\text{ for }k_x=\omega/v_D, \quad \text{(S36)}$$

$$(u_1,u_2,u_3,u_4)^T_{(-x)}=e^{-i\pi/4}(-i,1,i,-1)^T/2\text{ for }k_x=-\omega/v_D. \quad \text{(S37)}$$

The zero-frequency mode defined by the mass vortex winding resides on the same sublattice as in (S33): $(u_b,u_a,v_a,v_b)^T(\rho)=e^{-|m_{\mathrm{c}}|\rho}(1,0,0,i)^T/\sqrt{2}$. Similarly, it can now be decomposed into the valley-Hall edge modes, bearing spin-flip upon reflections from the opposite edges at $|x|=\rho_0$:

$$\hat{U}_{\mathrm{ab}}^{-1}\begin{pmatrix} u_b \\ u_a \\ v_a \\ v_b \end{pmatrix}(\omega=0)=\frac{1}{\sqrt{2}}\hat{U}_{\mathrm{ab}}^{-1}\begin{pmatrix} 1 \\ 0 \\ 0 \\ i \end{pmatrix}=\frac{1}{2}\begin{pmatrix} -i \\ -i \\ i \\ i \end{pmatrix}=\begin{pmatrix} u_1 \\ u_2 \\ u_3 \\ u_4 \end{pmatrix}(\omega=0,|x|<\rho_0) \tag{S28}$$

$$\propto \frac{e^{-\frac{i\pi}{4}}}{2}\begin{pmatrix} 1 \\ -i \\ -1 \\ i \end{pmatrix}+\frac{e^{-\frac{i\pi}{4}}}{2}\begin{pmatrix} -i \\ 1 \\ i \\ -1 \end{pmatrix}=\frac{1}{2}\left(1+\hat{U}_{\mathrm{ab}}^{-1}\hat{R}_M(-\pi)\hat{R}_k(-\pi)\hat{U}_{\mathrm{ab}}\right)e^{-i\pi/4}\begin{pmatrix} 1 \\ -i \\ -1 \\ i \end{pmatrix}.$$

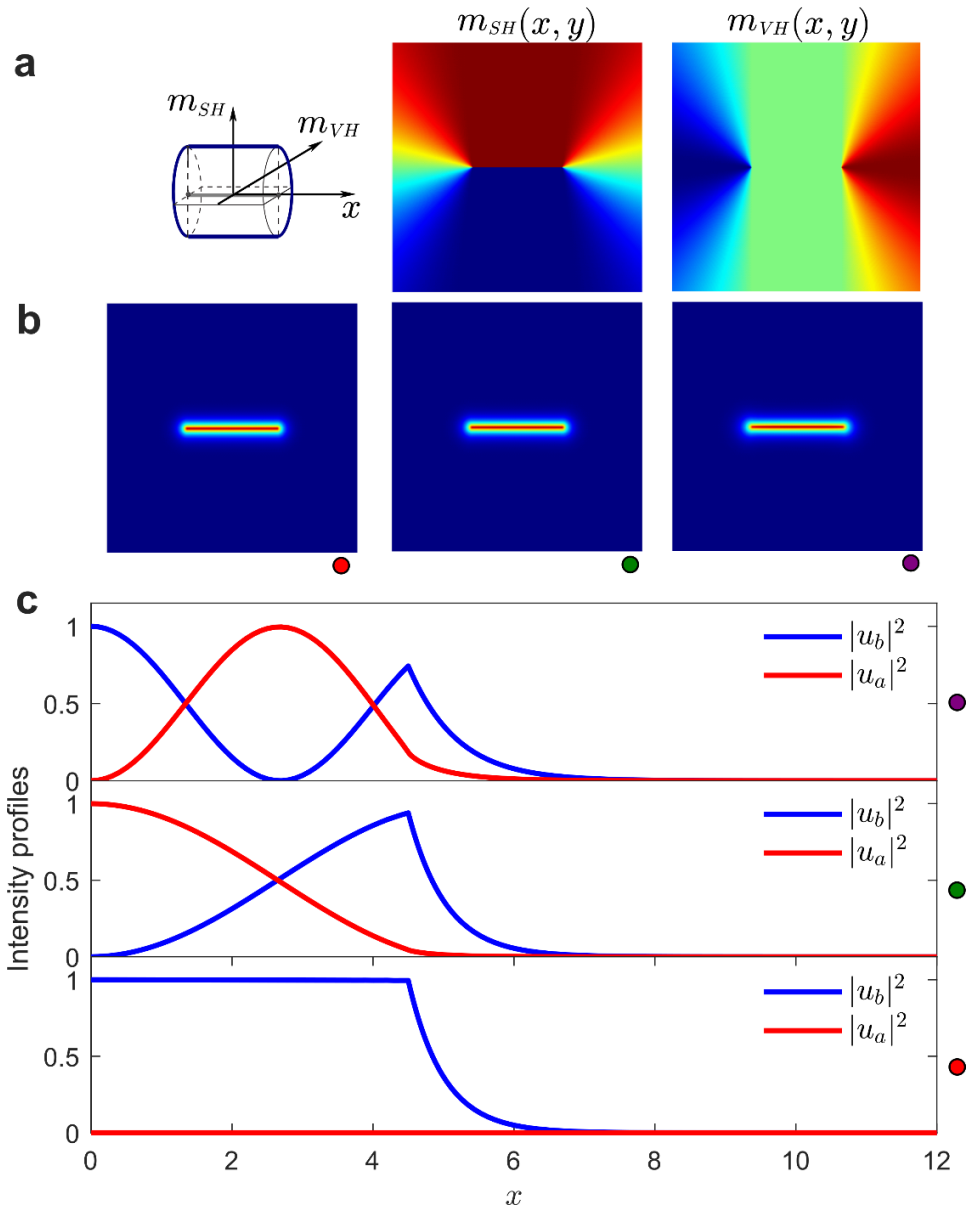

Fig. S2. Modes of the line-defect cavity. a, Schematic of the mass winding (left, dark blue curve) pooled from $-\rho_0$ to ρ_0 along the x axis and mass distribution m_{SH} (middle) and m_{VH} (right) in the xy plane. **b**, Representative intensity images for three pill-shape modes at the frequencies $\omega = 0$ (red dot), $\omega = 0.29629$ (green dot), $\omega = 0.58589$ (purple dot). **c**, Corresponding profiles of the components $|u_a| = |v_a|$, $|u_b| = |v_b|$ at $y = 0$ aligned with the defect. Parameters $v_D = 1$, $m_c = 1$, $\rho_0 = 4.5$.

Supplementary References

1. Kawaguchi, Y. et al. Pseudo-spin switches and Aharonov–Bohm effect for topological boundary modes. *Sci. Adv.* **10**, eadn6095 (2024).
2. Gao, X. et al. Dirac-vortex topological cavities. *Nat. Nanotechnol.* **15**, 1012 (2020).
3. Smirnova, D. et al. Polaritonic states trapped by topological defects. *Nat. Commun*. **15**, 6355 (2024).
4. Kawaguchi, Y. et al. Geometric phase resonators (*manuscript in preparation*).